Histol Histopathol (2010) 25: 1507-1517
DOI: 10.14670/HH-25.1507

http://www.hh.um.es

Histology and Histopathology
Cellular and Molecular Biology

Histological differences in healing following experimental transmural infarction in rats

Jure Aljinović, Katarina Vukojević, Vana Košta, Maja Marinović Guić, Mirna Saraga-Babić and Ivica Grković
Department of Anatomy, Histology and Embryology, School of Medicine, Split, Croatia

Summary. Mechanisms of cardiac regeneration following transmural myocardial infarction were analysed in rat hearts using immunohistochemistry for α-SMA, caspase-3, Ki-67 and nestin markers. Seven weeks after experimental myocardial infarction, two different types of healing processes were revealed in rats with and without aneurysmatic bulging of the left ventricular wall.

Besides thinning of the ventricular wall, three zones characterized both types of scars: the scar zone (divided into central and peripheral parts), the peri-infarct zone and the border zone. The main difference between the types of scars was the presence of a central necrotic zone inside the aneurysmatic wall, while connective tissue with myofibroblasts characterized the same zone in non-bulging wall. Apoptotic caspase-3 positive cells were found in the granulation tissue of the border zone in aneurysmatic scar, while in non-bulging scar they characterized all three zones. Proliferating Ki-67 positive cells displayed reverse expression pattern compared to apoptotic cells. Quantification of α-SMA positive cells revealed 60% α-SMA positive cells inside the central part of the aneurysmatic scar zone and 39% in invaginating areas, versus 19% in non-invaginating areas of the peripheral zone, but only 30% in the peripheral part of the non-bulging scar zone. Nestin positive cells were found in both types of scars, but with different distribution. These results suggest that even seven weeks after myocardial infarction, the healing processes in non-bulging scars are in chronic phase, while aneurysmatic scars are still in subacute phase. Histological differences in scar healing might be important for functional properties of the heart wall and for heart recovery prognosis.

Key words: Myocardial infarction, α-SMA, Nestin, Ki-67, Caspase-3

Offprint requests to: Jure Aljinović. M.D., School of Medicine in Split, Šoltanska 2, 21000 Split, Croatia. e-mail: jure.aljinovic@mefst.hr

Introduction

Myocardial infarction (MI) is a result of a partial or complete blockage of a coronary artery flow producing an ischemia and subsequent segmental loss of cardiac myocytes (Kumar et al., 1992). There are two types of MI: subendocardial and transmural. Transmural infarction is a result of complete coronary artery occlusion affecting the whole thickness of the heart muscle (Kumar et al., 1992).

A well documented method of inducing MI (Fishbein et al., 1978a) is coronary ligation of the left anterior descending coronary artery (LAD). Although the pathogenesis of MI following the ligation of a coronary artery in rat and coronary artery disease in human is different, resultant histological evolution and scar formation are comparable (Fishbein et al., 1978b). The rat model is used because of minimal or absent collateral circulation in coronary vasculature, hence ligation usually results in a large transmural infarction with potential for aneurysm formation (Pfeffer et al., 1979; Oh et al., 2004).

The principle of healing in MI is the reparative fibrosis that prevents cardiac rupture (Sun and Weber, 2000). In the acute phase of infarction healing, necrotic tissue is removed by neutrophiles, macrophages and other inflammatory cells, followed by the subacute phase, characterized by the presence of granulation tissue. Myofibroblasts (myoFb) and endothelial cells proliferate and migrate into the infarcted zone where myoFb deposit collagen and cause contraction of the scar (Virag et al., 2007). In the chronic phase, granulation tissue is apoptotically transformed into thin and hypocellular collagenous scar, resulting in marked thinning of the left ventricular wall (Fishbein et al., 1978b). In humans, scar maturation takes approximately 7 weeks (Kumar et al., 1992) while in rats the necrotic tissue is completely replaced by connective tissue within 21 days (Fishbein et al., 1978b).

Left ventricular aneurysm (LVA) is an important

complication of transmural MI that bears great clinical significance because of high mortality (Yildirim et al., 2007). In human pathology LVA incidence ranges from 4%, if the definition of aneurysm is restricted to the outward pouching, or ballooning, of the segment of the left ventricular wall affected by the MI, to 40%, if akinesia or dyskinesia during systole is regarded as LVA (Davies, 1988). Total LAD occlusion increases the chance of aneurysm formation in humans by 3.1 fold (Yildirim et al., 2007). In rats there is a high incidence of aneurysm formation when the LAD is permanently ligated 2-3 mm from its origin (Sakaguchi et al., 2001). Aneurysms can develop in the early phase, when the acute infarct area rapidly stretches to form an aneurysm, or in later stages when the necrotic material is not completely infiltrated by fibrous tissue and aneurysm forms due to the weakness of recently formed collagen network (Davies, 1988; Castagnino et al., 1992). The description of histological changes in human aneurysms was first reported by Mallory et al. (1939) and described as a band of necrosis in the heart wall that remained there for a few months after the infarction (Mallory et al., 1939). Fishbein confirmed the persistence of necrotic bands in one of seven rats after the period of healing (Fishbein et al., 1978b), while Castagnino et al. (1992) hypothesized that failure of collagen network formation inside necrotic tissue is the main histological factor of aneurysm formation.

Cardiac regeneration is a complex mechanism of infiltration, proliferation, apoptosis, and dedifferentiation (Sun and Weber, 2000), established and investigated by using different histological markers.

Myofibroblasts at the infarct site can be detected by α-smooth muscle actin (α-SMA) (Fishbein et al., 1978b) and they are the principal cells for fibrogenesis and the transition of contractile behavior to the scar tissue through α-SMA microfilaments (Gabbiani, 1998; Sun and Weber, 2000). MyoFb appear on the third day in the infarct site and remain for months thereafter. α-SMA positivity is found only in smooth muscle cells of blood vessels in normal or non infarcted myocardium (Fishbein et al., 1978b).

Caspase-3 is an effector caspase that is considered useful for detection of apoptosis in MI (Samali et al., 1999). Although the occurrence of apoptosis is controversial in cardiomyocytes in subacute and chronic phases of MI (Takemura and Fujiwara, 2004), it has proven to be the main mechanism in which macrophages, myoFb, and endothelial cells are eliminated from the infarction (Takemura et al., 1998; Yaoita et al., 2000).

Ki-67 is a cell cycle-related protein expressed by proliferating cells in all phases of the active cell cycle (Sawhney and Hall, 1992). As a replication associated antigen, Ki-67 was never found in cardiomyocytes, suggesting that they undergo DNA repair instead (Takemura and Fujiwara, 2004). As for fibroblast and endothelial cells, their proliferation in mice peaked on the fourth day after ligation, slowed by the second week and ceased by the fourth week after MI (Virag and Murry, 2003).

The intermediate filament protein nestin is used as a marker for proliferating immature cells, suggesting its principal role in tissue regeneration (Wiese et al., 2004). It is also used as a biomarker to monitor stem cell-based activity underlying regenerative processes such as differentiation and proliferation (Scobioala et al., 2008). The up-regulation of nestin mRNA was found in the infarct border zone in humans, mice, and rats (El-Helou et al., 2005; Scobioala et al., 2008). Nestin positive cardiac stem cells are capable of differentiation into myocytes, neural progenitor cells and myoFb (Drapeau et al., 2005; El-Helou et al., 2005; Scobioala et al., 2008).

Currently, it is considered that scar is a living tissue, not just an acellular accumulation of collagen (Sun and Weber, 2000). An aneurysm is considered to be a complication of MI associated with a high mortality, and research on this subject is focused on its surgical removal and/or prevention of its incidence by early reperfusion (Sakaguchi et al., 2001). To the best of our knowledge there are no publications on the 'histological' process of healing in already formed aneurysms. Understanding the healing mechanisms inside an aneurysm is important in order to design therapeutic interventions aimed at improving cardiac recovery and prevention of heart failure.

Thus, we undertook this investigation in order to analyze healing processes at the cellular level in rats, 7 weeks after experimental transmural MI, with special emphasis on the comparison of differences in repair dynamics between transmural infarction with and without left ventricular aneurysm (ballooning of injured left ventricular wall).

Materials and methods

Animal model

All experimental protocols and procedures were approved by the Ethics Committee of the School of Medicine in Split and carried out according to laboratory animal guidelines (European Communities Council Directive of 24 November 1986). In this study we used Sprague-Dawley female rats (n=12) weighing 230-260 g. Animals were obtained from the Vivarium for experimental animals, University of Split, Croatia. The rats were housed in individual plastic cages in a temperature-controlled environment, maintained on a 12:12 hour light-dark cycle, with rat chow and water available ad libitum.

Rats where anesthetized with a mixture of Ketaminol (Ketaminol 10, 1.2 ml/kg, Intervet International, Netherlands) and Xylazinum (Xylapan, 0.4 ml/kg, Vetoquintol, Switzerland) injected in the right hamstring muscles. Endotracheal intubation was performed with an 18 gauge arterial catheter. We used the 'abdominal approach' to the heart (Huikeshoven et

al., 2000; Guic et al., 2010). The initial midline incision of the skin was followed by cutting the abdominal muscles. The xyphoid process was exposed; a knot was tied around it and lifted to get some tension on the diaphragm. With the aid of a surgical microscope (Leica, M520 MC1, Switzerland), medial section of the diaphragm was performed through both tendinous and muscular parts sparing phrenic vessels. Simultaneously with the diaphragm incision, rats were connected to an animal ventilator (SAR 830, CWE Inc, USA) set on 56 breaths/min and inspiratory pressure between 8 and 10 cm/H_2O. A self retaining retractor was used to widen the opening in the diaphragm. The pericardium was gently removed, the left side of the heart and left anterior descending coronary artery (LAD) were accessed by lifting the left auricle. We localized LAD by locating the corresponding vein on the surface of the heart between the left auricle and the pulmonary outflow tract. LAD is positioned deeper in the myocardium, just below the vein, and cannot be seen on the surface of the heart. The coronary vessels were ligated (with an 8.0 nylon suture) about 3 mm from their origin (Fig. 1), and the suture was secured using a drop of tissue contact glue (Superattak, Henkel Loctite, Ireland). The immediate colour change of the heart surface (pale appearance) was a sign of successful coronary ligation.

The diaphragm was sutured with a resorbable 6.0 suture starting at the muscular segment towards its tendinous part. After the air was expelled from the thoracic cavity, the final suture was tightened. At that point, animals were removed from the ventilator and resumed spontaneous respirations usually within one minute. Muscle layers and skin were sutured and animals were kept in a warm environment during the recovery period that lasted between 3 and 5 hours.

One animal died shortly after surgery due to massive infarction while three animals did not develop infarction. In seven animals, the hearts had visible macroscopic changes (colour, consistency) of the left ventricle (LV) corresponding to the transmural infarction and one rat had a balooning of the affected left ventricular wall. Representative hearts from transmural infarction with and without aneurysm (seven weeks after ligation), were further processed.

Tissue processing and histological staining

Rats were sacrificed and hearts were extracted and cut into two parts, dividing the atria from the ventricles. Ventricles were fixed in 4% paraformaldehyde in phosphate buffer and 15% saturated picric acid and dehydrated in 100% ethanol. Tissues were embedded in paraffin wax, serially sectioned (4-6 μm thick sections) and mounted on glass slides. After deparafinisation, sections were rehydrated in ethanol and water.

To detect infarcted areas and the anatomical relationship between different parts of the rat hearts, haematoxylin and eosin staining were performed.

For Mallory trichrome staining, sections were incubated with hematoxylin for 5 minutes, differentiated with tap water and treated afterwards with acid fuchsin for 1 minute. Following a few rinses with distilled water, sections were differentiated with 1% phosphomolybdic acid for 1 minute. After a brief rinse with distilled water, sections were stained with anilin blue for 15 minutes, again briefly rinsed with distilled water, differentiated with 1% acetic acid for 1-5 minutes and dehydrated in ethanol and xylol.

Sections for immunohistochemical staining were incubated for 10 min in 1% H_2O_2 to quench endogenous peroxidase activity and then washed in phosphate buffer saline (PBS). Sections for α-SMA and caspase-3 antibody staining were cooked in sodium citrate buffer (pH 6.0), whereas those for Ki-67 antibody staining were cooked in ethylenediaminetetraacetic acid (EDTA, pH 8.0) for 17 min at 95°C in a microwave oven.

After being cooled to room temperature, sections were incubated with goat serum (Normal Goat Serum, X0907 DAKO, Glostrup, Denmark) for 1 hour to block non-specific antibody binding. Afterwards, sections were separately incubated with monoclonal mouse anti-α-SMA primary antibody (dilution 1:150; M0851, Dako Denmark A\S, Denmark), polyclonal rabbit anti-Ki-67 antibody (1:100, AB9260, Chemicon, Temecula, CA, USA) and rabbit anti-caspase-3 antibody (1:1500, AF835, R&D sys, Minneapolis, USA) for 1 hour in a humidified chamber. Primary antibodies were diluted in Dako REAL antibody diluent (Dako Denmark A\S, Denmark). After being washed in PBS, primary antibodies were detected using a streptavidin-biotin peroxidase system (K0690, Dakocytomation, Carpinteria, Calif., USA) as recommended by the

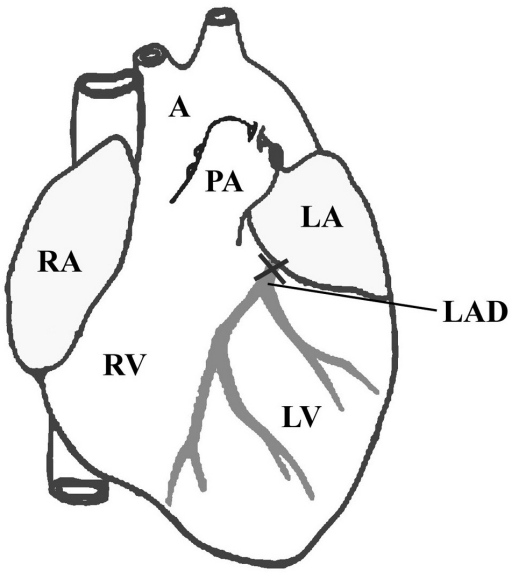

Fig. 1. Precise location of left anterior descending coronary artery (LAD) ligation in rat. Right ventricle (RV), right auricle (RA), left ventricle (LV), left auricle (LA), aorta (A), pulmonary artery (PA).

manufacturer, and then stained with diaminobenzidine tetrahydrochloride solution (DAB). Finally, the sections were rinsed in distilled water, counter-stained with haematoxylin, and dehydrated in ethanol and xylol. Cells positive to actin had brown-stained cytoplasm, while caspase 3-positive and Ki-67 positive cells had brown-stained nuclear signal.

Sections for immunofluorescence staining were treated in a microwave oven at 95°C for 17 minutes in sodium citrate buffer (pH 6.0). After being cooled to room temperature, sections were washed in PBS and incubated with goat serum (Normal Goat Serum, X0907 DAKO, Glostrup, Denmark) for 1 hour. After multiple washes in PBS, sections were incubated with mouse anti hNestin antibody (1:200, MAB1259, R&D systems, Minneapolis, USA) for 1 hour at room temperature. Thereafter, sections were rinsed in PBS and incubated for 1 hour with goat anti-mouse Rhodamine secondary antibody (1:200, AP124R, Jackson Immuno Research Lab., PA, USA).

Following secondary antibody incubation, the sections were washed in PBS and counterstained with DAPI to stain nuclei. Cells positive to nestin immunofluorescence had a diffuse red cytoplasmatic signal, while DAPI stained nucleus of all cells. Positive internal controls for actin staining were smooth muscle cells in vascular walls, and positive internal controls for nestin, Ki-67 and caspase 3 were other tissues that were known from the literature to stain abovementioned antibodies (Saraga-Babic et al., 2008; Vukojevic et al., 2009).

Staining controls included omission of primary antibodies from the staining procedure, which resulted in no staining of tissue. After final rinsing in PBS, all sections were mounted (Immuno-Mount, Shandon, Pittsburgh, PA, USA), air-dried and coverslipped. Immunolabeled tissues were viewed and photographed using an Olympus BX51 (Tokyo, Japan) microscope equipped with Olympus DP71 camera and processed with Cell A Imaging Software for Life Sciences Microscopy (Olympus Tokyo, Japan). Separate images were acquired for filters that allow visualization of DAPI and Rhodamine.

Quantification of α–SMA positivity

The number of α-SMA positive cells was evaluated quantitatively by two independent investigators and classified as negative (no stained cells) and positive (stained cells) cells. Counts were made throughout the whole diameter of the scar zone of hearts with and without a bulging aneurysm. For bulging aneurysms, central necrotic areas, non-invagination (Fig. 3C) and invagination zones (Fig. 3F), bordering necrotic tissue were separately counted, while in transmural infarction without a bulging aneurysm, the central (myofibroblast) zone and peripheral (fibrotic) zone were also separately quantitatively assessed (Fig 3E). DP-SOFT version 3.1 software was used to divide each chosen section of the heart wall in squares of 50x50μm at x20 magnification. Positive cell profiles were counted in squares that were completely covered with cells. The cells located on the left and upper border of squares were not taken into account, only those on the right and lower border. To avoid counting the same cell twice every third section was counted from the proximal, distal and middle part of the infarcted heart wall for each heart. Altogether we counted N=187, 50x50μm squares with 1892 cells analyzed. The percentage of α-SMA positive cells was calculated and expressed as a mean±SEM. For statistical comparison we used t-test (GraphPad Software, La Jolla, CA, USA) after we had confirmed normal distribution of the data. Significance was accepted at $p<0.05$.

Results

Seven weeks after infarction, cross sections of the whole rat hearts without wall bulging (Fig. 2A) and with aneurysmatic wall bulging (Fig. 2B) were stained by trichrome Mallory stain. In the scar area without wall bulging, increased collagen deposition (blue stain) was seen in the scar zone, the peri-infarct and the border zone (Fig. 2A). In the heart with a bulging aneurysm of the wall, the scar area was twice as long as the same area in the non-bulging heart, and characterized with minimal collagen deposition in the scar zone and the peri-infarct zone, as well as the border zone (Fig. 2B).

Hematoxylin and eosin staining

Histological examination of non-infarcted myocardium showed normal myocardial cells (cardiomyocytes) intermingling with connective tissue (endomysium) containing blood vessels (Fig. 3A). The area of transmural non-bulging infarction showed thinning of the cardiac wall with loss of cardiomyocytes, and an increase in the amount of fibrotic tissue present. The peri-infarct zone displayed proliferation of highly cellular connective tissue (granulation tissue) with numerous blood vessels, thus separating the scar from the epicardium and endocardium. The border zone (the zone of transition from the scar area to normal myocardium) was characterized by the emergence of granulation tissue with numerous blood vessels (Fig. 3B). In the area of transmural infarction with aneurysmatic bulging of the wall, the thinning of the wall was even more evident. Even at lower magnifications it was easily noticeable that the infarction zone contained a wide necrotic area surrounded by abundant granulation tissue and blood vessels, but lacked development of fibrotic tissue. The same granulation-type tissue was observed in the border zone (Fig. 3C).

Trichrome Mallory stain

The trichrome stain of non-infarcted myocardium revealed normal cardiomyocytes and a small amount of

connective tissue (endomysium) (Fig. 3D). The non-bulging scar zone and the peri-infarct area were predominantly composed of dense collagen fibers, having a typical wavy course. The middle part of the scar zone was occupied by the spindle shaped cells, corresponding to myofibroblasts (Fig. 3E). In the heart with a bulging aneurysm of the ventricular wall, the scar zone and the peri-infarct area had different histological characteristics when compared to the non-bulging scar. Here, the middle part of the scar still contained necrotic amorphous detritus, surrounded by highly cellular connective tissue with numerous blood vessels (granulation tissue). In addition, the amount of collagen deposition was much smaller when compared to the non-bulging scar, while at several places highly cellular strand of connective tissues penetrated the necrotic zone in the form of small invaginations (Fig. 3F).

α-smooth actin stain (α-SMA)

α-SMA stain of the normal myocardium revealed the presence of that marker only in the walls of blood vessels inside the endomysium (Fig. 3G). The scar zone and the peri-infarct area of the non-bulging wall showed an intense staining of spindle-shaped myofibroblasts within both the fibrotic scar and in the walls of blood vessels inside and around the scar tissue (the peri-infarct zone). Parts of the scar tissue contained dense connective tissue fibers with fibroblasts (Fig. 3H). The α–actin positive cells and granulation tissue were also seen in the border zone.

The scar area of the bulging wall displayed the centrally positioned non-cellular necrotic tissue, with myofibroblasts located only on the surface of the necrotic zone. In several places, invaginations of granulation connective tissue (predominantly composed of myofibroblasts) invaded the necrotic zone, while dense connective tissue fibers were missing (Fig. 3I). Abundant granulation tissue with α–actin positive cells was also seen in the border zone.

In rat with a bulging aneurysm, the mean number of cells counted in 50x50μm squares was 13.74±0.52 (N=84) and it was statistically higher (*t*-test, p<0.0001) than in rats without a bulging aneurysm 7.165±0.21 (N=103).

Statistically significant differences of proportion of α-SMA positive cells in aneurysmatic rat hearts was observed inside invagination areas of peripheral scar zone surrounding necrotic zones 0.39±0.03 (N=53) in comparison to the rest of the peripheral scar zone which was in contact with a necrotic area 0.19±0.02 (N=31) (*t*-test, p<0.0001). There were no α-SMA positive cells inside the central (necrotic) part of the scar zone (Fig. 4). In rat without a bulging aneurysm the central scar area had a statistically higher proportion of α-SMA positive cells 0.621±0.04 (N=44) than the peripheral fibrous area inside the scar zone 0.307±0.03 (N=59) (*t*-test, p<0.0001) (Fig. 4).

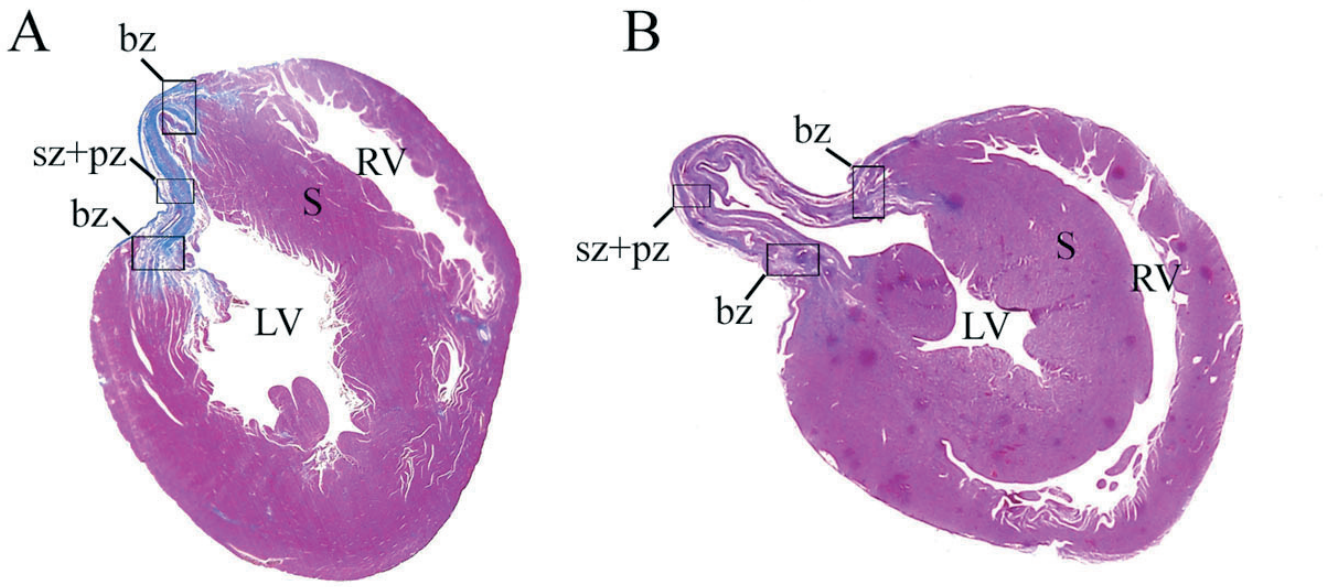

Fig. 2. Trichrome Mallory staining of cross sections of the two representative hearts following transmural infarction. **A.** Development of myocardial scar, without bulging of the left ventricular wall into the aneurysm. **B.** Development of myocardial scar, with bulging of the left ventricular wall into the aneurysm. Scar zone and peri-infarct zones (sz+pz), border zone (bz), left ventricle (LV), right ventricle (RV), interventricular septum (S). Myocardial scar is represented by blue stain, while the surviving myocardium is red.

Ki-67 proliferation marker

The area of normal myocardium displayed Ki-67 positive cells only occasionally in the endomysium, but not in the cardiomyocytes (Fig. 5A). The scar area in the wall of the non-bulging heart showed a moderate number of Ki-67 positive proliferating cells in the walls of blood vessels and inside the cells of newly formed connective tissue around the scar (the peri-infarct zone) and in the border zone of non-infarcted myocardium (Fig. 5B).

The scar area of the bulging heart wall contained numerous Ki-67 proliferating cells in the connective tissue and blood vessels (granulation tissue) coating the necrotic tissue, particularly in places of invaginations into the necrotic zone (Fig. 5C). Numerous proliferating cells were also found in the border zone.

Caspase-3

Normal myocardial tissue did not show any signs of caspase-3 activity, either in the connective tissue or in the cardiomyocytes (Fig. 5D). In the non-bulging scar area, caspase-3 positive cells were only occasionally found within the scar zone, between the myofibroblasts and fibrotic tissue (Fig. 5E). In the wall of a bulging

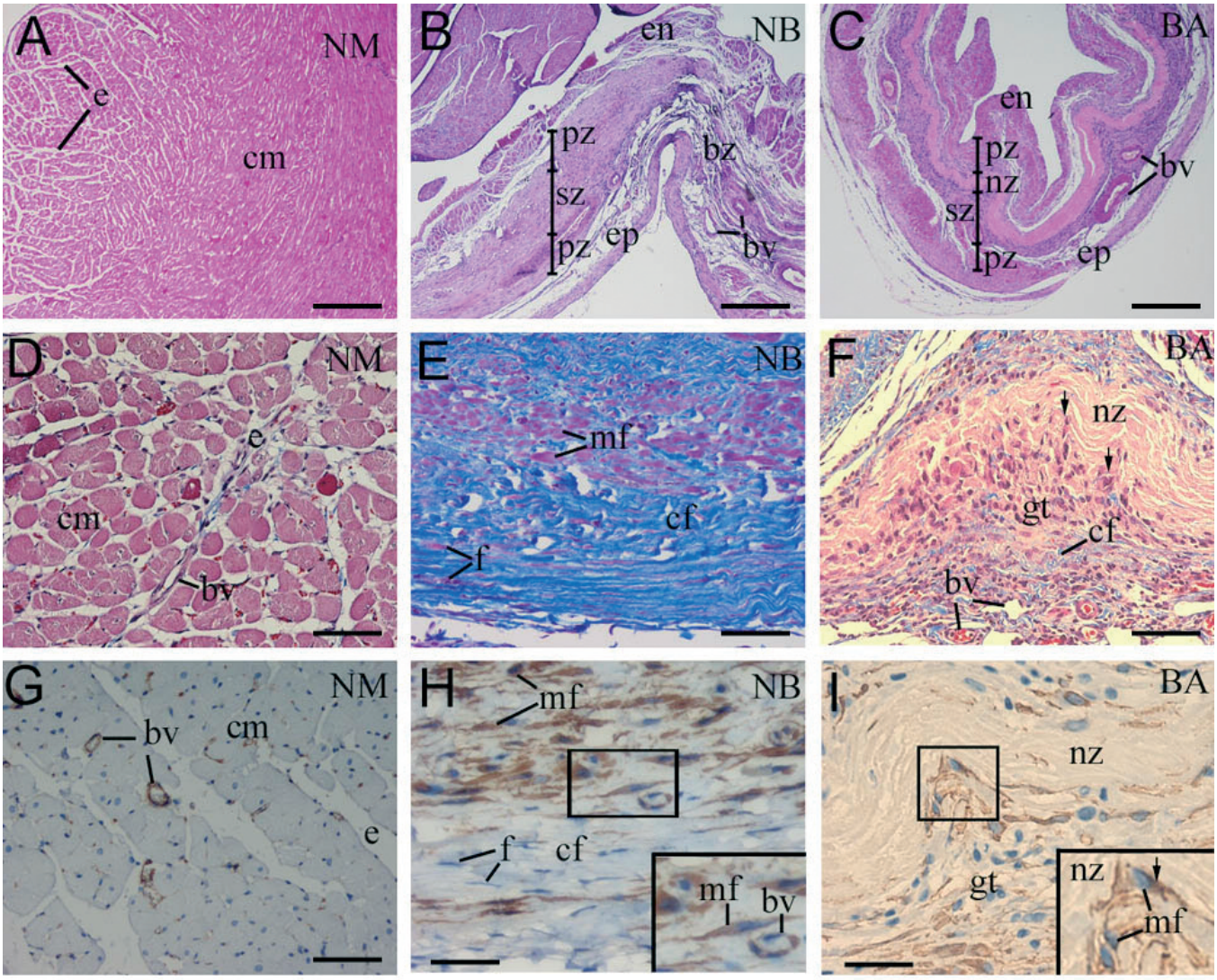

Fig. 3. Histological sections comparing features of normal myocardium (NM) with transmural infarction scar areas of non-bulging (NB) and bulging aneurysmatic (BA) heart stained by Hematoxylin&Eosin (A-C), trichrome Mallory stain (D-F), α-SMA stain (G-I). Cardiomyocytes (cm), endomysium (e), scar zone (sz), peri-infarct zone (pz), border zone (bz), necrotic zone (nz), endocardium (en), epicardium (ep), granulation tissue (gt), invaginations of granulation tissue (arrows), myofibroblasts (mf), fibroblast nuclei (f), collagen fibers (cf), blood vessels (bv). Scale bars: A-C, 250 μm; D-F, 50 μm; G-I, 25 μm; insert in I, x 100.

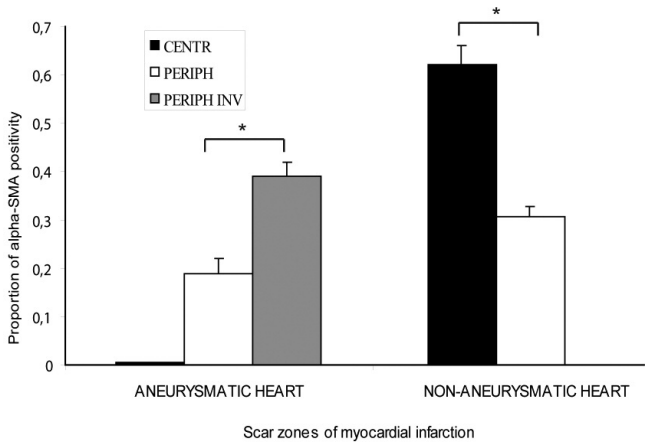

Fig. 4. Proportion of α-smooth muscle actin in scar zones of aneurysmatic and non-aneurysmatic hearts. Central scar zone (CENTR), peripheral scar zone (PERIPH), areas of localized invagination of mitotically active cells inside peripheral zone in aneurysmatic heart (PERIPH INV). The asterisk indicates a significant difference at $p<0.05$.

aneurysm, the area of necrotic tissue and the peri-infarct zone were completely devoid of caspase-3 positive cells. They were present only in the granulation-type connective tissue cells and in the walls of blood vessels of the border zone (Fig. 5F).

Double immunofluorescence staining with nestin and DAPI

DAPI staining was used in order to detect orientation of cell nuclei inside the scar. In the scar area of the wall of the non-bulging heart, nestin positivity was identified in the cytoplasm of several cells inside the scar zone (Fig. 6A), while staining with DAPI disclosed parallel orientation of cell nuclei in the scar area (Fig. 6B). Cellular profiles positive to both nestin and DAPI nuclear stain displayed spindle shape characteristics resembling myofibroblasts (Fig. 6C). Scar area of the bulging aneurysm: invaginations of granulation tissue penetrating the necrotic zone displayed intense nestin reactivity in the cytoplasm of several cells in the vicinity of the necrotic zone (Fig. 6D), while DAPI stain was detected in numerous, irregularly scattered nuclei (Fig. 6E). After merging, it became obvious that most of the cells in the invagination areas were nestin positive and spindle shaped cells. A total lack of cellular profiles, as

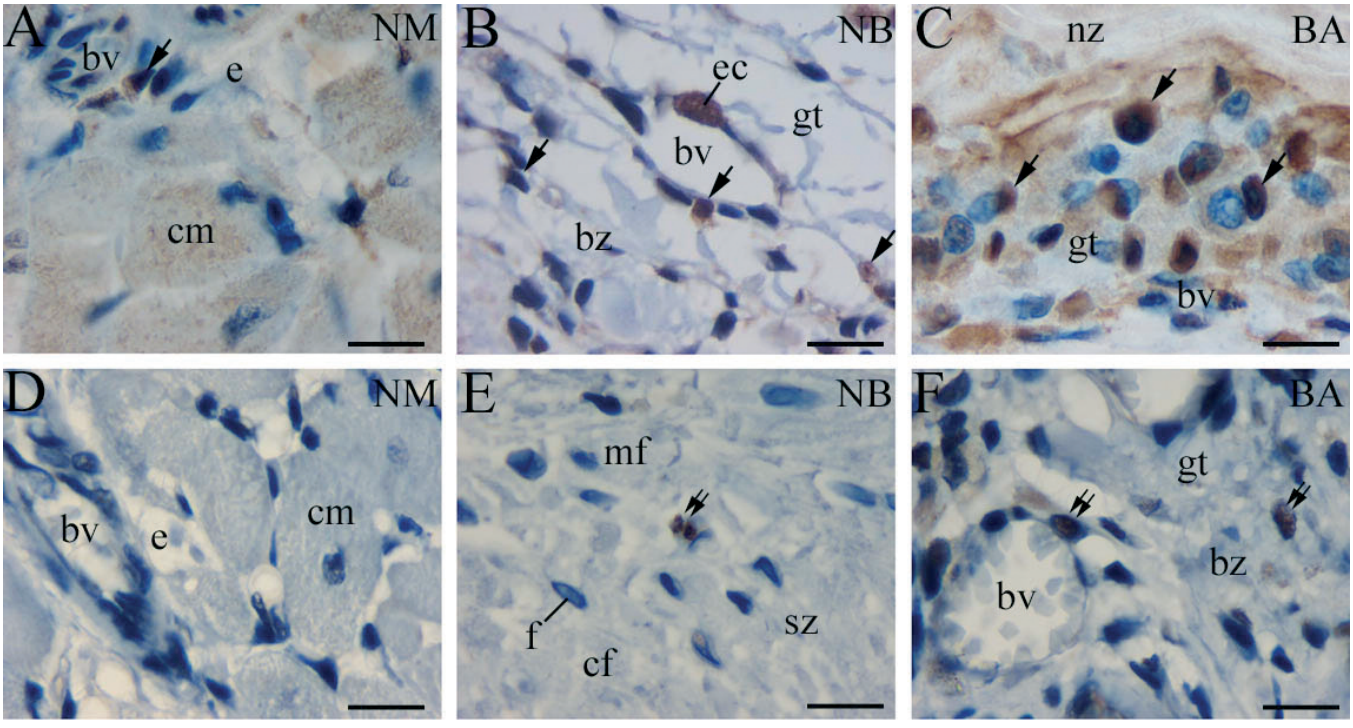

Fig. 5. Comparison of proliferation and apoptotic processes in normal myocardium (NM) with transmural infarction scarring areas of non-bulging (NB) and bulging aneurysmatic (BA) hearts. Nuclei of proliferating cells are marked by arrows, nuclei of apoptotic cells with double arrows. Scar zone (sz), border zone (bz), cardiomyocytes (cm), endomysium (e), blood vessels (bv), granulation tissue (gt), necrotic tissue (nt), endothelial cells (ec), fibroblast nuclei (f), myofibroblasts (mf), collagen fibers (cf). Immunostaining to Ki-67 (A-C), and caspase-3 (D-F), Scale bars: 10 μm.

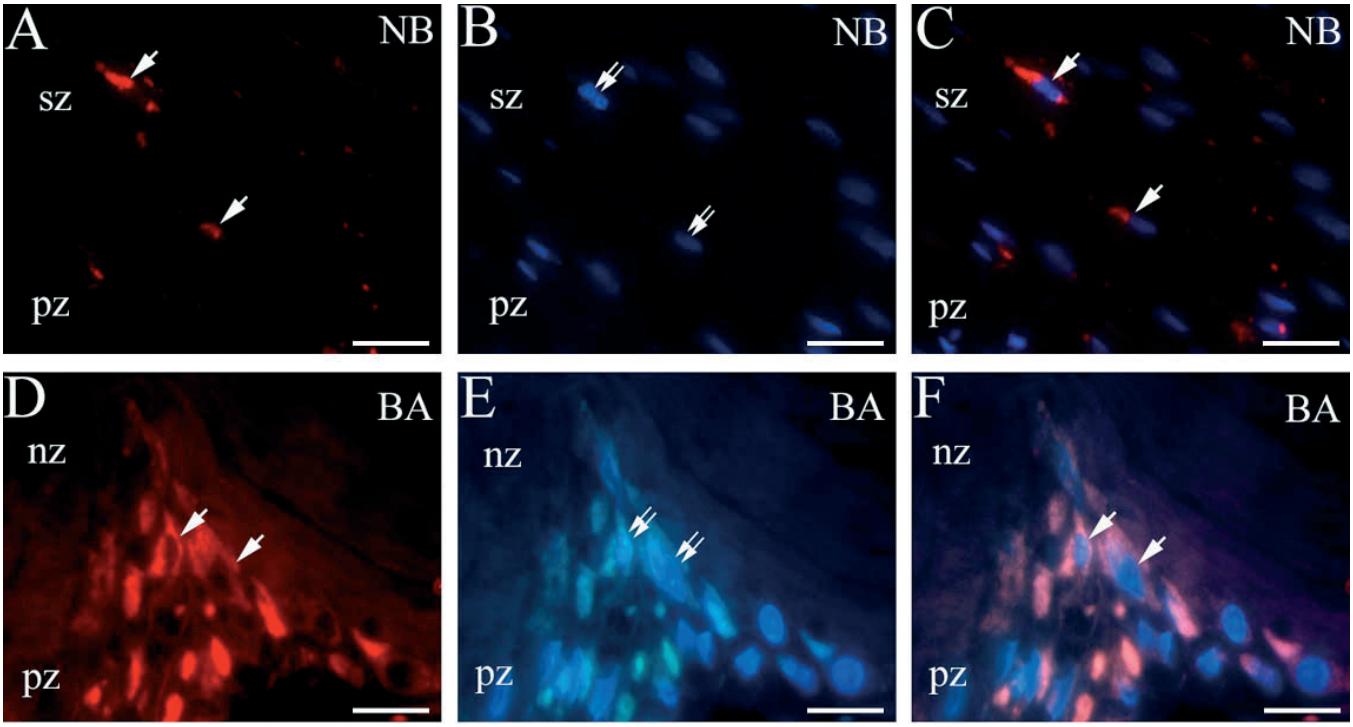

Fig. 6. Distibution of nestin positive cells in non-bulging (NB) and bulging aneurysmatic (BA) heart walls. Nestin-positive cells (arrows) located between scar zone (sz) and peri infarct zone (pz) of non-bulging (NB) heart wall (**A**), and between necrotic zone (nz) and peri infarct zone (pz) of bulging aneurysmatic (BA) heart wall (**D**). DAPI nuclear staining (double arrows) of non-bulging (**B**) and bulging (**E**) heart wall. Merging of nestin and DAPI staining (arrows) (**C, F**). Double immunofluorescent stain. Scale bars: A-C, 25 μm; D-F, 15 μm.

well as the absence of staining for any of the markers used, was characteristic for the necrotic zone (Fig. 6F).

Discussion

In all experimentally induced transmural infarcts, the hearts displayed macroscopically noticeable thinning of the ventricular wall. In one of them, a large bulging of the left ventricular heart wall developed, resembling an aneurysm, representing a late complication of infarction. The thinning of the wall was associated with necrosis of cardiomyocytes, as previously described in the literature (Fishbein et al., 1978b; Pfeffer et al., 1979).

Histological analysis of the two types of post-infarct scars included scar with transmural infarction followed by bulging of the heart wall (aneurysm) and others without bulging of the heart wall (non-bulging). Our results disclosed clear histological differences in the late (chronic) tissue reactions. Apart from differences in the extent of the affected area (the aneurysmatic wall had a scar twice as long as the non-bulging scar), the main characteristic of the scar in the aneurysmatic heart was a wide necrotic zone, while in the non-aneurysmatic scar the necrotic zone was replaced by fibrous tissue. Previous investigations also described persistence of a necrotic zone, abundant granulation tissue and absence of fibrous infiltration of the entire wall of the aneurysm (Fishbein et al., 1978a; Castagnino et al., 1992), which is in agreement with our findings. It has been reported that larger infarcts take longer to heal (Miura et al., 1991). In humans, some infarcts have a central area of necrosis persisting for a long period of time, extending the healing period (Fishbein et al., 1978a). In dogs, the necrotic material is removed by neutrophils, followed by macrophages (Frangogiannis et al., 2000). Although the principles of necrosis removal have similar histological patterns in humans and in rats, the polimorphonuclear component appears to be unusually mild and brief in rats (Fishbein et al., 1978a; Frangogiannis et al., 2000; Virag et al., 2007). It is well known that the presence of a necrotic zone represents a high risk for cardiac rupture. Although it was proven that replacement of necrotic tissue with collagen lowers the risk for rupture in aneurysmatic hearts, the mortality from heart failure remains high (Davies, 1988). In our study, the investigated MI scars histologically consisted of three distinct zones: 1) a scar zone containing necrosis and granulation tissue in the aneurysmatic heart, or central myofibroblast area and peripheral fibrous area in the non-anurysmatic heart, 2) a peri infarct zone with granulation tissue separating the scar from endocard and epicard, and 3) a border zone that represents a transitional region separating the non-infarcted myocardium from the myocardial infarction zone.

Differences in the time needed for maturation of the scar, represented by the transfer of granulation tissue into collagenous scar, vary signifficantly, from 3 weeks in rats (Fishbein et al., 1978b) to 6-8 weeks in humans (Kumar et al., 1992). Closer histological insight into the non-aneurysmatic scar revealed abundant fibrous and granulation tissue, as well as the presence of myoFb inside the scar and in the peri-infarct zone. However, in the aneurysmatic scar, the fibrotic tissue (collagen network) was rare, while the central necrotic area was surrounded by abundant granulation tissue and myoFb found only in invaginations of granulation tissue, which continued into the peri-infarct zone without a clear demarcation line. In the border zone, the aneurysmatic heart contained numerous myoFb, while their quantity was moderate in the same area of the non-aneurysmatic scar. Thus, the maturation of the aneurysmatic wall was delayed in comparison to the non-aneurysmatic wall. Differences in the two healing patterns described above were also confirmed with the finding of a statistically higher number of cells in aneurysmatic than in non aneurysmatic hearts, suggesting that the process of healing inside the aneurysm was still in the subacute phase, unlike the non-aneurysmatic heart, which at that time already reached the chronic phase of healing.

In normal myocardium, myoFb were found only in the walls of blood vessels. It was reported that in mice, in the first two weeks after infarction, myoFb were replicated at the border zone and migrated towards the peri-infact area. The second possible mechanism for myoFb appearance at the infarct site could be the dedifferentiation of fibroblasts, leading to the expression of markers for immature smooth muscle cells, such as SMemb (isoform of myosin heavy chain) and α-SMA (Frangogiannis et al., 2000). The possible function of myoFb includes the contraction of scar tissue using their microfilament connections with extracellular matrix and with each other (Sun and Weber, 2000). However, by the fourth week, myoFb were reported to be restricted only to the wall of the blood vessels (as in normal heart) due to apoptosis or their down regulation (Virag and Murry, 2003). Those finding were not in agreement with our results, because we found myoFb in scar tissue even seven weeks after infarction in both non-aneurysmatic and aneurysmatic hearts. In non-aneurysmatic heart, myoFb were primarily located in the central scar zone, while they were less numerous in the peripheral scar zone, but their typical distribution probably enabled constant tension on the scar. Previous investigations pointed to a 40-50% reduction in infarct size of rat and dog models, partially due to the above mentioned mechanism (Virag et al., 2007). Contrary to this, the unorganized collagen network is found in the aneurysmatic heart and absence of myoFb in the necrotic zone caused inefficient contraction of the scar, and thus its size remained the same (Castagnino et al., 1992).

Processes of cell proliferation and apoptosis are considered to be essential for scar remodeling (Takemura et al., 1998). In mice, proliferation of endothelial and fibroblast cells peaked at day four after ligation, slowed down after two weeks and ceased after four weeks of ligation (Virag and Murry, 2003), while in rats the process was even shorter (Jugdutt et al., 1996). Our investigation established that even in the 7th week following transmural infarction, proliferation was still very active, particularly in the peri-infarct and border zones of the aneurysmatic heart (where numerous proliferating cells were visible in contact with remaining necrotic tissue), as well as in the endothelial cells of blood vessels inside granulation tissue. On the other hand, the proliferation process had already ceased in the scar and peri-infarct region, but was still active in the border zone of non-aneurysmatic hearts.

Different numbers and distribution of apoptotic cells were detected in the two types of scar healing: in the aneurysmatic heart, caspase-3 positive apoptotic cells were found only in granulation tissue of the border zone, while in the non-aneurysmatic heart those cells were distributed in all three zones (scar zone, peri-infarct and border zone). Apoptosis was not detected in cardiomyocytes, but was confirmed in granulation tissue cells. A lack of apoptotic cells in the aneurysmatic heart might be a sign that the subacute phase was still active, and pro-apoptotic signals were not sufficiently expressed to enable cleansing of granulation tissue, while apoptosis in the non-aneurysmatic heart might represent the final organization of scar tissue (Takemura et al., 1998; Yaoita et al., 2000).

In human cardiac tissue, the number of apoptotic cardiomyocyte cells in MI is detected by TUNEL and immunohistochemistry, and varies significantly in the literature from 0.05 to 35% (Takemura and Fujiwara, 2004). DNA fragmentation studies and studies of nuclear ultrastructure confirmed that apoptosis is the mechanism of clearing of granulation tissue (myoFb, macrophages, endothelial cells) following the subacute phase of infarction (Takemura et al., 1998). Therapeutic prevention of apoptosis by caspase inhibition showed controversial results: in some studies causing a reduced size of infarction, while in others it showed no effect (Yaoita et al., 2000; Takemura and Fujiwara, 2004). Considering our results, we could speculate that caspase inhibiton in the chronic phase of infarction healing has very little influence on cardiomyocyte preservation, even in the aneurysmatic heart, since we did not find any apoptotic cells in the scar zone.

We have found the presence of immature cells that expressed nestin inside the scar and in the peri-infarct region of non-aneurysmatic hearts, and only in the peri-infarct zone of the aneurysmatic heart, mostly situated around necrotic tissue and newly formed vessels. By now, nestin positivity has been confirmed in endothelial cells and cardiac fibroblasts (Scobioala et al., 2008), with a recent discovery of a subpopulation of nestin positive cells that might be considered cardiac stem cells (Drapeau et al., 2005; El-Helou et al., 2005; Scobioala et al., 2008). It is believed that cardiac stem cells have limited proliferation but broad differentiation potential,

including neuronal progenitor cells (Wiese et al., 2004). Neuronal progenitor cells have been reported to cause sympathetic hyperinnervation in the areas of increased repair, and possibly leading to malignant arrhythmias (Hasan et al., 2006). In our study, nestin positivity was expressed in the aneurysmatic heart in a few areas that directly contacted necrotic tissue, but not along the full length of the necrotic zone. That is in agreement with findings suggesting that their number might not be sufficient for effective healing (Scobioala et al., 2008). Transplantations of bone marrow stem cells to the infarcted area were performed in order to limit the size of the infarct (Orlic et al., 2001). Investigations on possible pathways of nestin cell differentiation and their roles in the process of post-infarct scar healing are the focus of our ongoing studies.

Acknowledgements. The authors thank Mrs. Asija Miletić for her skilful technical assistance and Prof. Damir Sapunar for provision of secondary antibody Rhodamin. This study was funded by the Ministry of Science, Education and Sports, Republic of Croatia (Project no. 216-2160528-0067) and (Project no. 021-2160528-0507) whose support is gratefully acknowledged.

References

Castagnino H.E., Toranzos F.A., Milei J., Weiss V., Beigelman R., Sarchi M.I., Bordenave C.A. and Azcoaga R. (1992). Preservation of the myocardial collagen framework by human growth hormone in experimental infarctions and reduction in the incidence of ventricular aneurysms. Int. J. Cardiol. 35, 101-114.

Davies M.J. (1988). Ischaemic ventricular aneurysms: true or false? Br. Heart. J. 60, 95-97.

Drapeau J., El-Helou V., Clement R., Bel-Hadj S., Gosselin H., Trudeau L.E., Villeneuve L. and Calderone A. (2005). Nestin-expressing neural stem cells identified in the scar following myocardial infarction. J. Cell. Physiol. 204, 51-62.

El-Helou V., Dupuis J., Proulx C., Drapeau J., Clement R., Gosselin H., Villeneuve L., Manganas L. and Calderone A. (2005). Resident nestin+ neural-like cells and fibers are detected in normal and damaged rat myocardium. Hypertension 46, 1219-1225.

Fishbein M.C., Maclean D. and Maroko P.R. (1978a). Experimental myocardial infarction in the rat: qualitative and quantitative changes during pathologic evolution. Am. J. Pathol. 90, 57-70.

Fishbein M.C., Maclean D. and Maroko P.R. (1978b). The histopathologic evolution of myocardial infarction. Chest 73, 843-849.

Frangogiannis N.G., Michael L.H. and Entman M.L. (2000). Myofibroblasts in reperfused myocardial infarcts express the embryonic form of smooth muscle myosin heavy chain (SMemb). Cardiovasc. Res. 48, 89-100.

Gabbiani G. (1998). Evolution and clinical implications of the myofibroblast concept. Cardiovasc. Res. 38, 545-548.

Guic M.M., Kosta V., Aljinovic J., Sapunar D. and Grkovic I. (2010). Characterization of spinal afferent neurons projecting to different chambers of the rat heart. Neurosci. Lett. 469, 314-318.

Hasan W., Jama A., Donohue T., Wernli G., Onyszchuk G., Al-Hafez B., Bilgen M. and Smith P.G. (2006). Sympathetic hyperinnervation and inflammatory cell NGF synthesis following myocardial infarction in rats. Brain. Res. 1124, 142-154.

Huikeshoven M., van den Brink A. and Beek J.F. (2000). Alternative surgical exposure of the rat heart in vivo using a simple abdominal approach. Eur. Surg. Res. 32, 368-373.

Jugdutt B.I., Joljart M.J. and Khan M.I. (1996). Rate of collagen deposition during healing and ventricular remodeling after myocardial infarction in rat and dog models. Circulation 94, 94-101.

Kumar V., Cotran R.S. and Robbins S.L. (1992). Basic pathology. 5th ed. W.B. Saunders company. Philadelphia, Pennsylvania.

Mallory G., White P. and Salcedo-Salgar J. (1939). The speed of healing of myocardial infarction: A study of the pathologic anatomy in seventy-two cases. Am. Heart J. 18, 647-671.

Miura T., Shizukuda Y., Ogawa S., Ishimoto R. and Iimura O. (1991). Effects of early and later reperfusion on healing speed of experimental myocardial infarct. Can. J. Cardiol. 7, 146-154.

Oh Y.S., Thomson L.E., Fishbein M.C., Berman D.S., Sharifi B. and Chen P.S. (2004). Scar formation after ischemic myocardial injury in MRL mice. Cardiovasc. Pathol. 13, 203-206.

Orlic D., Kajstura J., Chimenti S., Jakoniuk I., Anderson S.M., Li B., Pickel J., McKay R., Nadal-Ginard B., Bodine D.M., Leri A. and Anversa P. (2001). Bone marrow cells regenerate infarcted myocardium. Nature 410, 701-705.

Pfeffer M.A., Pfeffer J.M., Fishbein M.C., Fletcher P.J., Spadaro J., Kloner R.A. and Braunwald E. (1979). Myocardial infarct size and ventricular function in rats. Circ. Res. 44, 503-512.

Sakaguchi G., Young R.L., Komeda M., Yamanaka K., Buxton B.F. and Louis W.J. (2001). Left ventricular aneurysm repair in rats: structural, functional, and molecular consequences. J. Thorac. Cardiovasc. Surg. 121, 750-761.

Samali A., Zhivotovsky B., Jones D., Nagata S. and Orrenius S. (1999). Apoptosis: cell death defined by caspase activation. Cell. Death Differ. 6, 495-496.

Saraga-Babic M., Bazina M., Vukojevic K., Bocina I. and Stefanovic V. (2008). Involvement of pro-apoptotic and anti-apoptotic factors in the early development of the human pituitary gland. Histol. Histopathol. 23, 1259-1268.

Sawhney N. and Hall P.A. (1992). Ki67--structure, function, and new antibodies. J. Pathol. 168, 161-162.

Scobioala S., Klocke R., Kuhlmann M., Tian W., Hasib L., Milting H., Koenig S., Stelljes M., El-Banayosy A., Tenderich G., Michel G., Breithardt G. and Nikol S. (2008). Up-regulation of nestin in the infarcted myocardium potentially indicates differentiation of resident cardiac stem cells into various lineages including cardiomyocytes. FASEB. J. 22, 1021-1031.

Sun Y. and Weber K.T. (2000). Infarct scar: a dynamic tissue. Cardiovasc. Res. 46, 250-256.

Takemura G. and Fujiwara H. (2004). Role of apoptosis in remodeling after myocardial infarction. Pharmacol. Ther. 104, 1-16.

Takemura G., Ohno M., Hayakawa Y., Misao J., Kanoh M., Ohno A., Uno Y., Minatoguchi S., Fujiwara T. and Fujiwara H. (1998). Role of apoptosis in the disappearance of infiltrated and proliferated interstitial cells after myocardial infarction. Circ. Res. 82, 1130-1138.

Virag J.I. and Murry C.E. (2003). Myofibroblast and endothelial cell proliferation during murine myocardial infarct repair. Am. J. Pathol. 163, 2433-2440.

Virag J.A., Rolle M.L., Reece J., Hardouin S., Feigl E.O. and Murry C.E. (2007). Fibroblast growth factor-2 regulates myocardial infarct repair:

effects on cell proliferation, scar contraction, and ventricular function. Am. J. Pathol. 171, 1431-1440.

Vukojevic K., Skobic H. and Saraga-Babic M. (2009). Proliferation and differentiation of glial and neuronal progenitors in the development of human spinal ganglia. Differentiation 78, 91-98.

Wiese C., Rolletschek A., Kania G., Blyszczuk P., Tarasov K.V., Tarasova Y., Wersto R.P., Boheler K.R. and Wobus A.M. (2004). Nestin expression--a property of multi-lineage progenitor cells? Cell. Mol. Life Sci. 61, 2510-2522.

Yaoita H., Ogawa K., Maehara K. and Maruyama Y. (2000). Apoptosis in relevant clinical situations: contribution of apoptosis in myocardial infarction. Cardiovasc. Res. 45, 630-641.

Yildirim A., Soylu O., Dagdeviren B., Eksik A. and Tezel T. (2007). Sympathetic overactivity in patients with left ventricular aneurysm in early period after anterior myocardial infarction: does sympathetic activity predict aneurysm formation? Angiology 58, 275-282.

Accepted May 19, 2010